Proceedings of the 2015 Winter Simulation Conference
L. Yilmaz, W. K. V. Chan, I. Moon, T. M. K. Roeder, C. Macal, and M. D. Rossetti, eds.

SCHOOL CLOSURE STRATEGIES FOR THE 2009 HONG KONG H1N1 INFLUENZA PANDEMIC

Zoie Shui-Yee Wong

School of Public Health and Community Medicine
University of New South Wales
UNSW Sydney 2052, AUSTRALIA

David Goldsman

School of Industrial and Systems Engineering
Georgia Institute of Technology
Atlanta, GA 30332-0205, U.S.A.

Kwok-Leung Tsui

Department of Systems Engineering and Engineering Management
City University of Hong Kong
Kowloon Tong, HONG KONG

ABSTRACT

Modelling of detailed community interaction dynamics increases a public health organization's ability to contain a potential disease strain at an early stage. Due to its dense population and high levels of human movements and interactions, Hong Kong has suffered from various epidemic diseases. The use of non-medical interventions is often efficacious in containing pandemic outbreaks. In this paper, we focus on evaluating the effectiveness of various practical school-related non-medical intervention strategies to mitigate the effects of pandemic influenza under a realistic Hong Kong demographic scenario. We modelled the impact of a combination of various school closure modes, triggers, types, and lengths. The simulation results suggest that the strategy of closing all types of schools generally outperforms that of closing only a subset, especially if the closure period is substantial. We also discuss future research directions along with individual school closure and economic evaluations.

1 INTRODUCTION

Effective and timely reactive strategies bring tremendous benefits with respect to pandemic disease response. The Asia-Pacific region, particularly the southern part of China, is often the epicenter of emerging infectious diseases, having given rise to recent outbreaks. According to the CIA World Factbook, the population in Mainland China (including Hong Kong (HK)) is about 1.3 billion, which constitutes about 20% of the world's population, and the urban-rural ratio is about 50-50% (CIA 2015). People living in urban areas are constantly in close contact, and urban populations experience a vastly different lifestyle than suburban populaces. Hong Kong, as the economic and logistics center of Asia, has a population of more than 7 million residents along with a significant floating population in its limited domestic landmass of 1,000 square kilometers. Due to its dense population and its economic and financial status, Hong Kong has become a place that is susceptible to epidemic diseases, e.g., H5N1 in 1997 (Chan 2002), SARS in 2003 (Riley et al. 2003), Swine flu in 2009 (Wu et al. 2010), Avian flu, etc. Increased population density and mobility can magnify the spread of emerging infectious diseases and can potentially lead to an outbreak. The good news is that modelling of detailed community interaction dynamics increases a public health organization's ability to contain a potential strain at its origin.

The ability to decide effective and timely strategies that help contain pandemics of transmissible diseases such as influenza is of great importance to government policy makers and healthcare professionals. Although these recommendations are generally applicable to all cities/countries, regional differences in demographic characteristics may affect the effectiveness of such recommended strategies. In the past, various articles have been dedicated to the development of synthetic populations and contact networks for epidemiological models (Eubank et al., 2004 and 2006). Recently, a number of simulation-based studies have been conducted focusing on the evaluation of various reactive strategies to influenza spread. For instance, to investigate the role of targeted social distancing, such as school closure, in mitigating pandemic influenza in a small town in the United States, Glass et al. (2006) described a network-based simulation model for the influenza spread. Longini et al. (2004) used a stochastic epidemic simulation model to investigate the effectiveness of targeted antiviral prophylaxis to contain influenza in the United States. Longini et al. (2005) further extended the stochastic simulation model for rural Southeast Asia to investigate the effectiveness of targeted antiviral prophylaxis, quarantine, and pre-vaccination in containing an influenza strain at the source. Similarly, Ferguson et al. (2005) applied a simulation model of influenza transmission in Southeast Asia to evaluate the potential effectiveness of targeted mass prophylactic use of antiviral drugs as a containment strategy, as well as the effectiveness of other interventions aimed at reducing population contact rates.

There are two general types of intervention strategies: medical and non-medical. It has been suggested that studying interventions without antiviral use and vaccination is a useful exercise because (i) antivirals may not be effective against new outbreaks and (ii) an adequate vaccination supply might require a long time to be prepared (World Health Organization Writing Group 2006). With respect to non-pharmaceutical interventions, various studies have shown that school closure is an effective social distancing strategy (Mikolajczyk et al. 2008; Koomin and Cetron 2009), while in any case schools play an important role in past influenza outbreaks (Glass and Glass 2008). It has been shown that children are efficient transmitters of influenza, are more vulnerable to infection, and are at higher risk of infection consequences than adults (Tsui et al. 2013; Halder, Kelso, and Milne 2010). Lee et al. (2010) have also demonstrated that school closures could delay an epidemic peak and allow time for medical interventions, such as vaccination. A recent systematic review (Jackson et al., 2014) gives an extensive discussion on related school closure work using simulation models and points out that there is a lack of simulation studies that investigate the effectiveness of individual, regional, and national school closure strategies. In our preliminary study, we observed that strategies involving the school-closure intervention outperformed medical interventions (Chan, Wong, and Tsui 2014).

In the regional perspective, modelling detailed community dynamics provides a better opportunity to identify the spread of a pandemic influenza strain, especially at its beginning phase. Although various studies have pointed out that schools may be major environments of disease transmission, a carefully designed quantitative model is still needed to examine the effects of timely and proper school closure strategies. The current study was developed based on the pandemic influenza situation in 2009 for Hong Kong, and our research targets are twofold: (i) to develop a region-based simulation for Hong Kong that mimics the disease spread situation in 2009; and (ii) to evaluate the effectiveness of various school closure strategies based on attack rate outcomes, where attack rates are simply the percentages of children who ultimately acquire flu. Our work is based on the study of Andradóttir et al. (2011). Using the 2009 H1N1 pandemic situation in Hong Kong, we examine the effects of realistic school closure intervention strategies implemented after various periods on the progression of influenza outbreaks.

The remainder of this paper is organized as follows. Section 2 details our methodology, including various school closure strategies. Section 3 summarizes our results, and Section 4 presents a discussion, directions for future research, and conclusions.

2 METHODOLOGY

Section 2.1 provides a high-level summary of the 2009 H1N1 outbreak, discusses our model, and presents various school closure strategies. Section 2.2 gives details concerning model initialization, the calibrated baseline models, and sensitivity analysis.

2.1 Historical Process and Model Design

2.1.1 The H1N1 Outbreak in Hong Kong

The outbreak of a new swine-origin influenza A (H1N1) virus took place in Mexico in March/April 2009. The virus spread rapidly to 30 countries during the first few weeks of surveillance, and the World Health Organization (WHO) raised its pandemic alert to level 5 out of 6. In Hong Kong, the first indexed case, which was also the first confirmed case in Asia, was found on 1 May 2009, and subsequently Hong Kong's influenza pandemic alertness level was raised to "emergency" from "serious". The cumulative numbers of confirmed cases in HK since the first confirmed case are depicted in Figure 1. According to a recent WHO report, the virus spread worldwide to more than 214 countries and caused more than 18,000 deaths (WHO, 2010).

Our simulation is designed to mimic the effects of school closure strategies under the 2009 HK outbreak. The model was calibrated by taking into account the natural epidemiological history of H1N1 along with data and findings of the H1N1 pandemic in Hong Kong (Wu et al. 2010).

2.1.2 Age-stratified Regional-specific Disease-spread Simulation Model

We developed an age-structured regional-specific Susceptible-Exposed-Infected-Removed (SEIR) model to provide scientific justifications for various mitigation strategies regarding school closure for Hong Kong. Currently, many simulators fail to explain how infectious disease is transmitted in a regional context as they often neglect region-specific dynamics, including age demographics and population mobility. In metropolitan cities, the rapid movement of people from one community to another has the effect of spreading diseases within a short period. Based on Andradóttir et al. (2011), we developed an age-structured regional-specific SEIR model of pandemic influenza transmission based on population data from HK's Census and Statistics Department (Census and Statistics Department 2012). Unlike traditional influenza simulators that typically focus on large-scale populations with a generalized individual contact structure, the developed model realistically considers the disparities of demographic structures and regional dynamics across districts. Such a simulation allows for a finer level of detail for administrators to set up localized strategies, which, for example, can take into account the effects of individual school closures in one district based on regional triggers or thresholds, to counter the spread of infectious diseases dynamically.

The population used in our simulation study is a synthetic population created via a population generator (Chan, Wong, and Tsui 2012) based on the data from the Census and Statistics Department (2012). The generator inputs parameters at two levels: global and regional (district). Global parameters define global metadata such as age group definitions, household structures, and the number and sizes of districts. Parameters at the regional (district) level describe further details of various distributions such as age and household composition, number of schools by type, and number of district council constituency areas (DCCA). This approach incorporating multi-level details enabled us to accurately generate a synthetic population at a fine geographical level. The resulting synthetic population contains 6,888,600 agents representing the domestic population. Each agent processes a list of attributes with values that are stochastically generated: age, residential zone, household, community, neighborhood, and workplaces/schools with respect to the corresponding regional (district) parameters. Three types of educational institutions are defined: kindergartens (for preschool children aged 3–5), primary schools (for students aged 6–11), and secondary schools (for students aged 12–18) based on the actual demographics in Hong Kong. We employ a synthetic population because such necessary level of detail is unavailable from the public domain due to privacy issues. Figure 2 outlines the conceptual relationships of these contact places, that is, the places in which people can interact during the day.

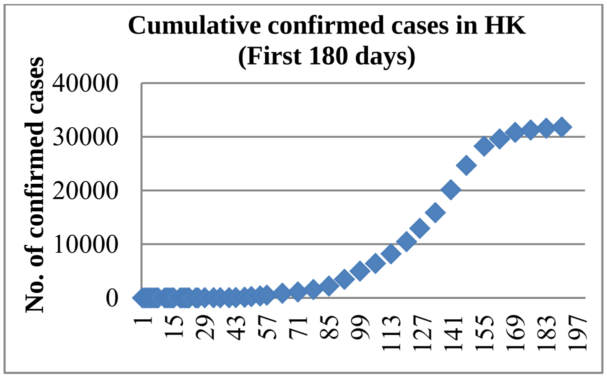

Figure 1: Cumulative number of confirmed cases in Hong Kong since first confirmed case on 1 May 2009 (Source: HSI Dashboard 2009).

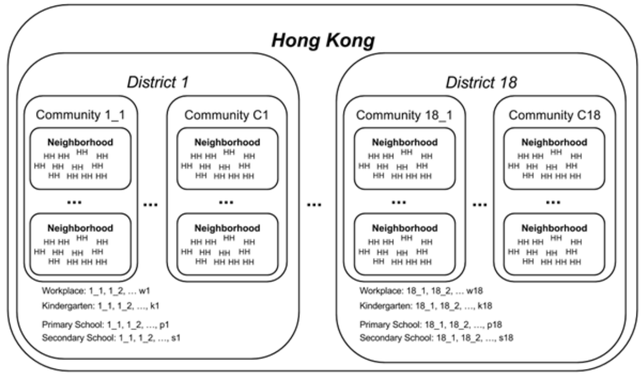

Figure 2: Hong Kong population model.

We adopted the well-known SEIR compartmental model, simulation flowchart, and natural history of influenza; see, e.g., Andradóttir et al. (2011). In our model, there are four types of contact places: households, communities, neighborhood areas (a neighborhood area is a subdivision of a community), and workplaces/schools. The probability *p* of a given susceptible individual becoming infected on a given day depends on the number of infectious people in the susceptible's contact groups, on the contact probabilities, and on the probability of transmission given contact. A simple Bernoulli(*p*) trial is conducted to determine if the susceptible is infected or not (where *p* varies from susceptible to susceptible). At the initialization phase, we introduced 100 infectious individuals and then added 10 more infectious individuals per day. The daily introduction of additional infectious individuals addresses the possibility of multiple introductions of the disease (Mills et al., 2006), and more-closely mimics the reality of infectives immigrating into the population from the outside. Furthermore, for some particularly effective intervention scenarios that reduce what is known as the basic reproduction number (R_0) (a measure of the potential of disease spread) to approximately 1, the disease may become extinct "too early" in some simulation runs. Introducing daily infectives better reflects the disease's epidemiological behavior in a city.

In order to model school children's activities more accurately, we specified the age for each agent and assigned their school type. With regard to the individuals, each agent is associated with the following generated attributes: age, household, kindergarten (for pre-school children aged 3–5), school attended (for children aged 5–18, including primary school and secondary school), workgroup (for working adults and working 15–18 year old children), community, and neighborhood (a subset of the community, e.g., major estates in HK). The characteristics of this model are as follows: (a) The homogeneous assumption of population structure is relaxed. We introduce a new district concept to explain population heterogeneities. Age distribution, household composition, workplaces, and educational institutions are dependent on district-specific distributions. (b) We model DCCA at the community level. Every day, each susceptible agent may be infected based on a size-dependent fractional exponent of full community contacts; and we further divide each DCCA into neighborhoods with an average size of about 500. A "contact count (CC)" parameter is introduced to realistically model possible daily contacts. (c) Population mobility at the district level is further detailed, which allows for cross-community activities for both students and workers across other areas in Hong Kong.

2.1.3 School Closure Strategies

We scrutinized the past history / news of government progress with regard to school closure decisions in Hong Kong and identified several strategies that are potentially implementable and practical for HK. We modelled a baseline case where no intervention takes place, along with strategies representing various combinations of schooling strategies, include examining the impacts of (1) mode of school closure (by type of school and by district), (2) school closure trigger, and (3) school closure length. Students only attending full-time education institutions were considered. Children younger than 3 years old were assumed to have contacts only at the household, community, and neighborhood levels. For each intervention strategy, the simulator conducts 20 runs from which age-stratified and overall illness attack rates can be captured. The following paragraphs briefly describe various school policy interventions that we consider.

2.1.3.1 School Type

School levels based on actual Hong Kong data definitions are identified and given as follows.

- Kindergarten (aged 3–5) (K)
- Primary school (aged 6–11) (P)
- Secondary school (aged 12–18) (S)

Considering students attending full-time education institutions, school sizes and student ratios on various school levels by districts were stratified according to the census data. For school closure strategies, schools of each level (K, P, and S) and the possible combinations (KP and KPS) were examined when a particular illness threshold is reached (the illness threshold will be elaborated in the next section).

2.1.3.2 Closure Modes

The simulation also runs various system-wide, district-wide, and individual school closure strategies. A school system closure strategy shuts down the entire school system once a certain trigger or threshold is reached. A district-wide closure strategy entails closure of the schools in the same district when the district illness threshold is reached. These strategies can be operated at the same time in practice. However, in this experiment, we use only a single strategy at a time.

2.1.3.3 School Closure Trigger

Different illness thresholds for initiating and terminating school closures were examined. For system-wide school closure, Lee et al. (2010) simulated rates of symptomatic cases of 0.10, 0.50, 1.00, or 1.50 percent of a 1.2 million person population. In HK, the first confirmed case was found on 1 May 2009, and the number of confirmed cases by the onset of day 180 was about 31,582 (less than 0.5% of the population); see Figure 1. The criteria for initiating and terminating school closures are as follows: Earliest closure triggers at a day, a week, and 2 weeks after the first case found are considered. Such delays could be interpreted as the time needed to resolve disagreements among officials conducting school closure decision-making. To realistically adjust to the practical situation in Hong Kong, our study sets triggers of 50, 100, 150, 200, and 300 confirmed cases within the population for system-wide school closure, assuming an ascertainment rate from symptomatic cases of 0.7. The ascertainment rate refers to the probability that a symptomatic case can actually be detected as a confirmed H1N1 case. Here is a summary of thresholds triggering interventions in a particular simulation run.

- First Confirmed Case Found with 1-day delay (FCF) – System-wide school closure
- First Confirmed Case Found with 1-week delay (FCF1) – System-wide school closure
- First Confirmed Case Found with 2-weeks delay (FCF2) – System-wide school closure
- Number of Confirmed Cases: 50, 100, 150, 200, 300 (NC) – System-wide school closure
- Number of Confirmed District Cases: 10, 20, 30, 50, 100 (NDC) – District-wide school closure

2.1.3.4 School Closure Length (SCL)

We found that increasing the duration of school closures can reduce the overall infection attack rate. However, school closure incurs high costs due to parents having to stay at home to look after their children. We assumed that school closure does not increase the per-contact probability of other contact groups, such as household, neighborhood, and community (Jackson et al. 2014). However, in reality the transmission rate in other contact groups might be affected due to school closure, for instance, if children are circulating more freely in the community. It has been a challenging problem to decide for how long schools should be closed using objective methods. In the 2009 HK H1N1 pandemic, the school closure length varied from 1 week to 2 weeks. In our study, we examined several school closure lengths (Araz et al. 2012), including 1, 2, 3, 4, 6, 8, and 16 weeks.

2.2 Model Initialization

2.2.1 Simulated Population

We generated individual characteristic distributions, such as age and place of work/study based on district level. In this Hong Kong model, children and adults are both permitted to attend a school / workplace outside the community that they belong to. The synthetic population contains 2,367,938 households, 394 communities, 13,562 neighborhoods, 147,125 workplaces, 976 kindergartens, 617 primary schools, and 531 secondary schools. Each agent was assigned unique group IDs based on their corresponding household, community, neighborhood, and school / workplace. These group contacts may overlap. For instance, two different households may belong to the same community and neighborhood, while two agents having different workplaces may belong to the same household. Table 1 summarizes our synthetic representation of Hong Kong (Chan, et al., 2012) side-by-side with the HK census data (Census and Statistics Department HKSAR, 2012).

Table 1: Comparison of simulated and census population structures.

Category	HK Simulated	HK Census
Domestic Population	6,888,600	6,890,476
District	18	18
Community	394 (avg. size ~17,483; CC* = 2000)	412 (avg. size ~16,724)
Neighborhood	13,562 (avg. size ~508)	N/A
Household	2,367,938 (avg. size ~2.9)	2,368,362 (avg. size ~2.9)
Workplace (age 15+)	147,125 (avg. size ~20)	N/A
Kindergarten (ages 3–5)	946 (avg. size ~166; CC* = 20)	976 (avg. size ~158)
Primary (ages 6–11)	572 (avg. size ~568; CC* =80)	617 (avg. size. ~578)
Secondary ages 12–18)	524 (avg. size ~891; CC* = 85)	531 (avg. size ~890)
Cross-community activities	Workgroup and School	Entire City

*We specify a contact count value to control the number of people that an individual will contact in the specific contact group. The CC is set to 20 for kindergarten, 80 for primary school, 85 for secondary school, 500 for neighborhood, and 2,000 for community in this simulation. People in households and workplaces are assumed to have full contact with the others.

Figures 3 and 4 display the marginal age distributions and marginal household size distributions for the simulated population and the true population obtained from census data. Based on these, we see that the distributions of age, household size, partial household composition, school groups, and work groups by districts based on the simulated population and census data are quite similar.

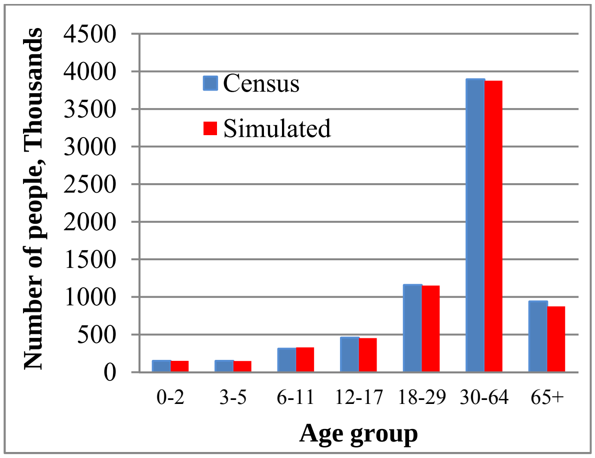

Figure 3: Marginal age distributions for a simulated population and the census data.

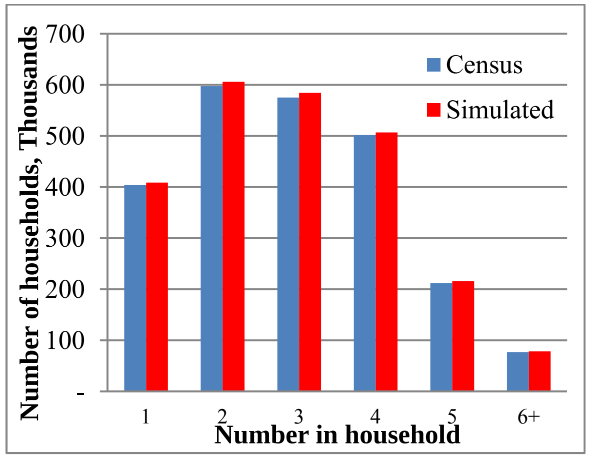

Figure 4: Marginal household size distributions for a simulated population and the census data.

2.2.2 Calibration and Sensitivity Analyses

We calibrated the age-group-specific cumulative infection attack rate (AR) at day 180 to match an independent study in Hong Kong; the target infection ARs for each age group can be referenced from Wu et al. (2010). The per-contact transmission probabilities as shown in Table 2 were tuned based on the suggested transmission probabilities in Andradóttir et al. (2011). The procedure is as follows: a set of rough upper bound parameter values based on 80% of the transmission probabilities and lower bound values based on 1% of the probabilities were first defined. Similar to Xu et al. (2004), an optimal three-level design with nine factors was carried out to search for appropriate values of each transmission parameter. We did not change the parameters within household and school / workplace at all since the household sizes were not greatly different from those of the previous models. A set of per-contact influenza infection transmission probabilities within contact groups was defined (as shown in Table 2) and an overall AR of 10.70% was achieved, which falls well within the target interval of 9.0 to 12.0% (Wu et al. 2010). The strength of transmission intensity can be reflected by the per-contact transmission probabilities for each contact group. We assumed heterogeneous transmissibility within schools depending on the student age group. In addition, all infection ARs in each age group fell within the 95% confidence intervals of the reported age-specific ARs of the pandemic (Wu et al. 2010). The basic reproduction number R_0 of the calibrated model was 1.1, which falls within the range of estimates between 1.1 and 2.1 for the 2009 H1N1 pandemic influenza (Pourbohloul et al. 2009).

Next, sensitivity analysis was undertaken by varying the percentage of coverage of antivirals from 1%, 2%, 5%, to 10% in various age groups and varying the percentage of coverage of vaccination from 1%, 5%, 10%, 20%, 30%, to 35% in various age groups. The results depicted in Figures 5 and 6 show a gradual decrease in the infection ARs when the percentages of coverage of antivirals and vaccination increase. Moreover, the same general transmission pattern manifests among all age groups, illustrating the robustness of those conclusions.

Table 2: Per-contact influenza infection transmission probabilities within contact groups.

Household		**Community**		**Neighborhood**	
Child-to-Child	0.08	Age 0–4	5E-8	Age 0–4	5E-7
Child-to-Adult	0.03	Age 5–9	5E-8	Age 5–9	5E-7
Adult-to-Child	0.03	Age 10–13	5E-8	Age 10–13	5E-7
Adult-to-Adult	0.04	Age 14–18	5E-8	Age 14–18	5E-7
Workgroups	0.01	Age 19–29	6E-5	Age 19–29	6E-4
Kindergarten	0.018	Age 30–52	7.5E-7	Age 30–52	7.5E-6
Primary school	0.0115	Age 53–64	5.5E-7	Age 53–64	5.5E-6
Secondary school	0.0065	Age 65+	5.5E-7	Age 65+	5.5E-6

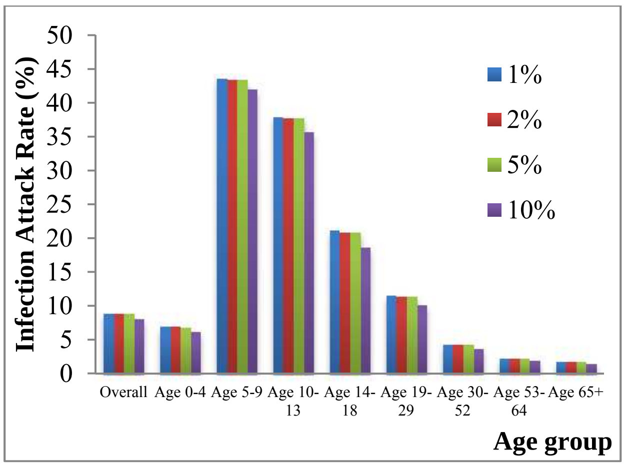

Figure 5: Sensitivity analysis for the coverage of antivirals.

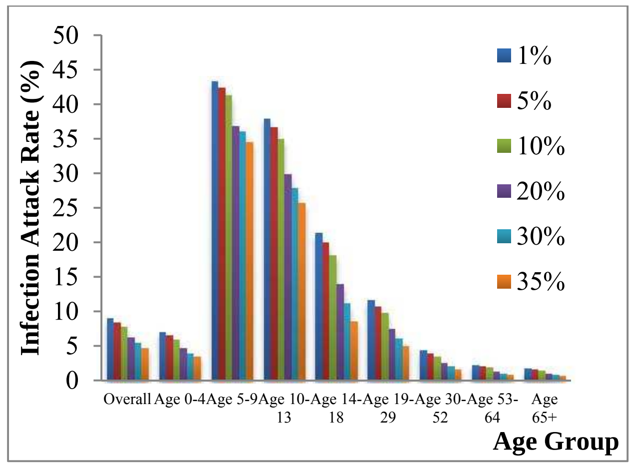

Figure 6: Sensitivity analysis for the coverage of vaccination.

3 RESULTS

This section reports on the simulation results and effectiveness of various school closure strategies. Figure 7 illustrates the simulation results based on triggers of the first case found date. We observe qualitatively similar overall attack rate patterns across different closure lengths among three different closure triggers (i.e., First Confirmed Case Found with 1-day delay (FCF), First Confirmed Case Found with 1-week delay (FCF1), and First Confirmed Case Found with 2-weeks delay (FCF2)). The effects of school closure based on the first case found trigger are not significant when the closure length is less than 6 weeks. In general, FCF2 performs better than FCF and FCF1, especially for longer closure lengths (such as 8 weeks). We observed a trend indicating that the school closure type makes a difference as the school closure length increases. When closure length is less than 8 weeks, the performance of the all school type closure (KPS) is slightly better than kindergarten and primary school only (KP), and KP performs slightly better than kindergarten closure only This trend became more obvious when school closure lengths are long (such as 8 weeks). The overall AR only drops to about 8% if school closure is in effect for 6 weeks and drops to about 7% if school closure is for 8 weeks. This observation generally applies to all tested closure triggers and is even more apparent in Figure 9, which is based on the number of confirmed *district* cases.

Figure 8 displays the simulated results for school system closure based on the number of confirmed cases in the entire city. Similar to Figure 7, closing more types of schools decreases the overall AR as the school closure length increases. In terms of the closure trigger, a larger trigger (such as 150, 200, and 300) has a stronger effect on disease transmission if all school types (KPS) are closed. This effect is not apparent when the school closing type is limited to kindergarten only and less apparent when setting a school closure type of kindergarten and primary.

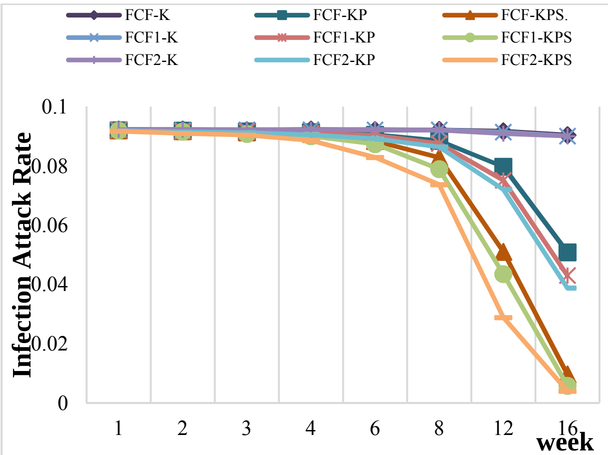

Figure 7: Closing schools after first case found (school system closure).

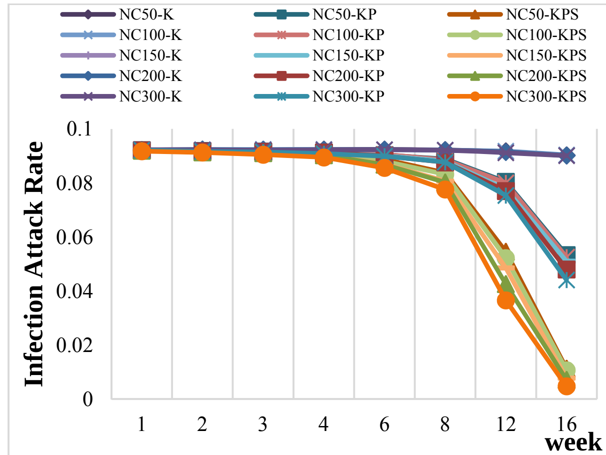

Figure 8: Closing schools based on the number of confirmed cases (for school system closure).

Figure 9 portrays the effects of school closure based on the number of confirmed district cases. This district-level closure illustrates that inclusion of more school types can reduce the overall ARs regardless of the closure trigger. The overall ARs drop dramatically as the closure period is increased from 4 weeks. Compared to the previous school closure strategies, this district-level closure strategy seems to result in a stronger effect on disease transmission. For the best scenario (i.e., NDC100-KPS), the overall AR drops to about 7% if school closure is for 6 weeks and drops to about 5% if school closure is for 8 weeks.

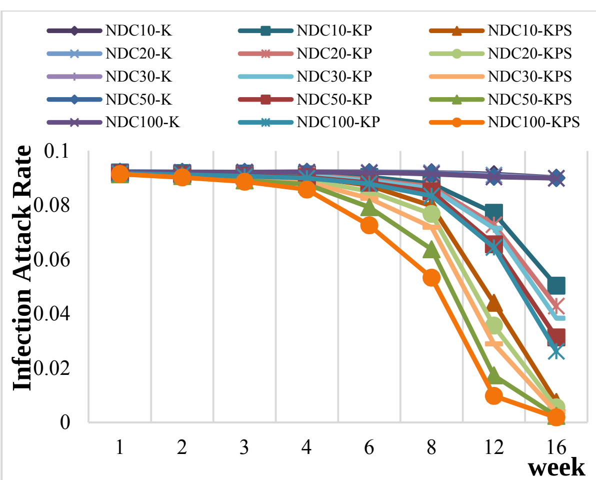

Figure 9: Closing schools based on the number of confirmed district cases (for district closure).

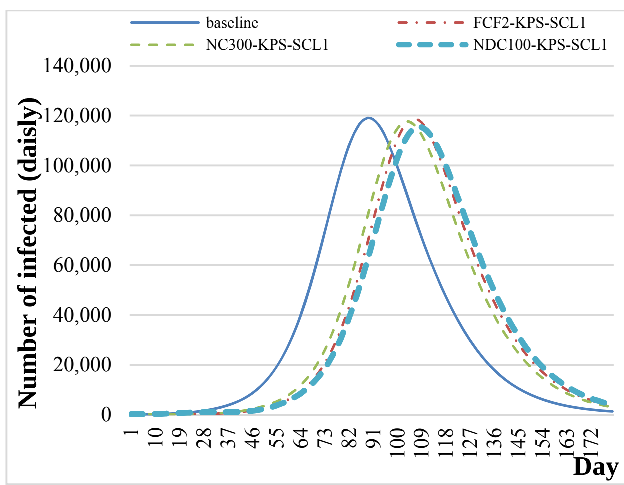

Figure 10: Epidemic curves of the baseline and selected school closure scenarios (SCL1).

The epidemic curve of H1N1 (i.e., the number of confirmed H1N1 cases over time) under selected closure strategies was compared to the baseline scenario (the unmitigated strategy) in order to understand the effects of intervention with respect to delaying the infectious disease spread. Our study predicted that closing schools would delay the epidemic peak vs. that of the baseline scenario. As shown in Figure 10, for a school closure period of 1 week, various scenarios (including FCF2-KPS, NC300-KPS, and

NDC100-KPS) can achieve 2 to 3 weeks delay of the epidemic peak compared to the baseline. Similar to other school closure studies, this study predicted that, in addition to occurring later, the peak was lower than in the unmitigated baseline scenario. For instance, NDC100-KPS with a closure length of 1 week achieved a 3% decrease compared to the unmitigated peak.

4 DISCUSSION, DIRECTIONS, AND CONCLUSIONS

This paper presented a simulation model of an influenza pandemic with a localized population structure, and evaluated various school closure intervention strategies using our simulation program. Based on our simulated outcomes, we found that closing more types of schools has the effect of better containing the spread of a disease, especially with increased school closure length. In general, the performance of all-school-type closure is better than kindergarten and primary schools only and certainly better than kindergarten closure only. Our simulation modeled cross-community activities of students and their effects when schools close. By limiting contact amongst students between schools, the overall attack rates can be reduced.

Our simulation program provides the flexibility to model school closure for specified types of schools based on various triggers. Future research will examine the effects of multiple school closure strategies. For instance, what is the combined effect of closing schools one week after the first case is found in conjunction with an individual school trigger of five cases across all types of schools?

We examined various system-wide and district-wide closure strategies. Future work can be focused on individual school closure, for instance, based on the number of confirmed cases at a particular school. Individual school closure may have promising results in relation to hindering the spread of disease effectively. Another direction to explore is to examine the effects of changing various school closure triggers, for instance, by examining the triggers of a higher number of confirmed cases both overall and at the district level. Moreover, the epidemic curve over time can be scrutinized and compared with the baseline scenario in order to understand the effects of interventions to delay the infectious disease spread. Future focuses can also be given to additional adjusting, calibrating, and validating models based on proven data and realistic school closure effects on containing pandemics. The attack rates of individual age groups will also be considered in order to determine better strategies for the targeted population.

School closure decisions are not trivial, may have uncertain consequences with respect to containing disease spread, and may also have significant social and economic impacts. For instance, closing school will put extra burdens on parents as they may be required to stay at home to take care of their children. Parents may have to take leave from work and lose income or even lose their jobs if the closure period is long. Some parents may possess critical skills (such as public health workers) that may inevitably affect smooth societal functioning. School closure may also cause disruptions to children's education and mental development as social and community services originating through school are disturbed. A future research direction will be to analyze economically the potential health benefits and economic losses incurred as we attempt to formulate an effective school closure policy for pandemics.

When preparing a responsive school closure policy in response to a potential influenza epidemic, public health policy makers and school administrators have to make judgments with respect to the pros and cons in terms of multiple dimensions (such as whether and when to close schools; how many schools to close; which schools to close; how long schools should close; and cost considerations). In the past, very few studies have provided sound metrics to guide such decision-making practically (i.e., down to a certain meaningful level of detail in a community). We envision an evidence-based approach that takes into account the system dynamics, the natural history of influenza, and the potential impact on various stakeholders that would be useful in determining the optimal intervention choices for purposes of mitigating an influenza epidemic.

ACKNOWLEDGMENTS

Our work was supported by the Research Fund for the Control of Infectious Diseases, granted by the Food and Health Bureau, HKSAR (Ref. 11101262), and the Collaborative Research Fund, granted by the Research Grants Council (Ref. CityU8/CRF/12G). We give special thanks to Mr. Hon Chan and Mr. Wei Huang for their support in coding and running scenarios of the simulation program.

REFERENCES

Andradóttir, S., W. Chiu, D. Goldsman, M. Lee, K. L. Tsui, B. Sander, D. N. Fisman, and A. Nizam. 2011. "Reactive Strategies for Containing Developing Outbreaks of Pandemic Influenza." *BMC Public Health* 11 (Suppl 1):S1, http://www.biomedcentral.com/1471-2458/11/S1/S1.

Araz, O. M., P. Damien, D. A. Paltiel, S. Burke, B. van de Geijn, A. Galvani, and L. A. Meyers. 2012. "Simulating School Closure Policies for Cost Effective Pandemic Decision Making." *BMC Public Health* 12(1):449–460.

Census and Statistics Department HKSAR 2012. Hong Kong 2011 Population Census Summary Results. http://www.censtatd.gov.hk/hkstat/sub/sp170.jsp?productCode=B1120055. Accessed April 4, 2015.

Chan, P. K. 2002. "Outbreak of Avian Influenza A (H5N1) Virus Infection in Hong Kong in 1997." *Clinical Infectious Diseases* 34(Supplement 2):S58–S64.

Chan, Y. H., Z. S. Y. Wong, and K. L. Tsui. 2012. "Synthetic Population – A Case Study of Hong Kong Population." *Proceedings of the IEEE International Conference on Industrial Engineering and Engineering Management (IEEM)*. 10–13 Dec. 2012, Hong Kong, China.

Chan, Y. H., Z. S. Y. Wong, and K. L. Tsui. 2014. "Modeling Influenza Pandemic in Hong Kong." *SCR-SEMS 2014*. 15–16 May 2014, Shenzhen, China.

CIA.gov. 2015. CIA Factbook – China. https://www.cia.gov/library/publications/the-world-factbook/geos/ch.html. Accessed June, 20 2015.

Eubank, S., H. Guclu, V. S. A. Kumar, M. V. Madhav, A. Srinivasan, Z. Toroczkai, and N. Wang. 2004. "Modelling Disease Outbreaks in Realistic Urban Social Networks." *Nature* 429:180–184.

Eubank, S., V. S. A. Kumar, M. Marathe, A. Srinivasan, and N. Wang. 2006. "Structure of Social Contact Networks and their Impact on Epidemics." *DIMACS Series in Discrete Mathematics and Theoretical Computer Science, Special Volume on Epidemiology* 70:181–213.

Ferguson, N. M., D. A. Cummings, S. Cauchemez, C. Fraser, S. Riley, A. Meeyai, S. Iamsirithaworn, and D. S. Burke. 2005. "Strategies for Containing an Emerging Influenza Pandemic in Southeast Asia." *Nature* 437(7056):209–214.

Glass, L. M. and R. J. Glass. 2008. "Social Contact Networks for the Spread of Pandemic Influenza in Children and Teenagers." *BMC Public Health* 8(1):61–75.

Halder, N., J. K. Kelso, and G. J. Milne. 2010. "Developing Guidelines for School Closure Interventions to be used During a Future Influenza Pandemic." *BMC Infectious Diseases* 10(1):221–234.

Hospital Authority HKSAR 2009. Special Human Swine Influenza Daily Dashboard. www.ha.org.hk/haho/ho/cico/3rdedition3rdMay2009.doc. Accessed 22 Jun 2015.

Jackson, C., P. Mangtani, J. Hawker, B. Olowokure, and E. Vynnycky. 2014. "The Effects of School Closures on Influenza Outbreaks and Pandemics: Systematic Review of Simulation Studies." *PLOS ONE* 9(5): e97297.

Koonin, L. M. and M. S. Cetron. 2009. "School Closure to Reduce Influenza Transmission." *Emerging Infectious Diseases* 15(1):137–138.

Lee, B. Y., S. T. Brown, P. Cooley, M. A. Potter, W. D. Wheaton, R. E. Voorhees, S. Stebbins, J. J. Grefenstette, S. M. Zimmer, R. Zimmerman, et al. 2010. "Simulating School Closure Strategies to Mitigate an Influenza Epidemic." *Journal of Public Health Management and Practice* 16(3):252–261.

Longini, I. M., M. E. Halloran, A. Nizam, and Y. Yang. 2004. "Containing Pandemic Influenza with Antiviral Agents." *American Journal of Epidemiology* 159(7):623–633.

Longini, I. M., A. Nizam, S. Xu, K. Ungchusak, W. Hanshaoworakul, D. A. Cummings, and M. E. Halloran. 2005. "Containing Pandemic Influenza at the Source." *Science* 309(5737):1083–1087.

Mikolajczyk, R., M. Akmatov, S. Rastin, and M. Kretzschmar. 2008. "Social Contacts of School Children and the Transmission of Respiratory-spread Pathogens." *Epidemiology and Infection* 136(06):813–822.

Mills, C. E., J. M. Robins, C. T. Bergstrom, and M. Lipsitch. 2006. "Pandemic Influenza: Risk of Multiple Introductions and the Need to Prepare for Them." *PLoS Medicine* 3(6): e135.

Pourbohloul, B., A. Ahued, B. Davoudi, R. Meza, L. A. Meyers, D. M. Skowronski, I. Villaseñor, F. Galvan, P. Cravioto, D. J. Earn, et al. 2009. "Initial Human Transmission Dynamics of the Pandemic (H1N1) 2009 Virus in North America." *Influenza and Other Respiratory Viruses* 3(5):215–222.

Riley, S., C. Fraser, C. A. Donnelly, A. C. Ghani, L. J. Abu-Raddad, A. J. Hedley, G. M. Leung, L.-M. Ho, T. H. Lam, T. Q. Thach, et al. 2003. "Transmission Dynamics of the Etiological Agent of SARS in Hong Kong: Impact of Public Health Interventions." *Science* 300(5627):1961–1966.

Tsui, K. L., Z. S. Y. Wong, D. Goldsman, and M. Edesess. 2013. "Tracking Infectious Disease Spread for Global Pandemic Containment." *IEEE Intelligent Systems* 28(6):60–64.

World Health Organization. 2010. Pandemic (H1N1) 2009 – update 100. http://www.who.int/csr/don/2010_05_14/en/. Accessed July 27, 2014.

World Health Organization Writing Group. 2006. "Nonpharmaceutical Interventions for Pandemic Influenza, National and Community Measures." *Emerging Infectious Diseases* 12:88–94. http://dx.doi.org/10.3201/eid1201.051371. DOI: 10.3201/eid1201.051371

Wu, J. T., E. S. Ma, C. K. Lee, D. K. Chu, P. L. Ho, A. L. Shen, A. Ho, I. F. Hung, S. Riley, L. M. Ho, et al. 2010. "The Infection Attack Rate and Severity of 2009 Pandemic H1N1 Influenza in Hong Kong." *Clinical Infectious Diseases* 51(10):1184–1191.

Xu, H., S. W. Cheng, and C. Wu. 2004. "Optimal Projective Three-level Designs for Factor Screening and Interaction Detection." *Technometrics* 46(3):280–292.

AUTHOR BIOGRAPHIES

ZOIE SHUI-YEE WONG is a Postdoctoral Research Fellow at the School of Public Health and Community Medicine at University of New South Wales. She was a Scientific Officer in the Centre for Systems Informatics Engineering (CSIE) at the City University of Hong Kong and was the recipient of Japan Society for the Promotion of Science (JSPS) Postdoctoral Fellowships for Foreign Researchers at the University of Tokyo. Her research focuses on disease-spread simulation, healthcare simulation, health systems engineering, and health informatics. Her contact e-mail address is zoiesywong@gmail.com.

DAVID GOLDSMAN is a Professor in the School of Industrial and Systems Engineering at the Georgia Institute of Technology. His research interests include simulation output analysis, ranking and selection, and healthcare simulation. He is a Fellow of the Institute of Industrial Engineers. His email address is sman@gatech.edu and his webpage is www.isye.gatech.edu/~sman.

KWOK-LEUNG TSUI is Chair Professor of Industrial Engineering and Department Head in the Department of Systems Engineering and Engineering Management at the City University of Hong Kong. He is also Director of the Centre for Systems Informatics Engineering. His email address is kltsui@cityu.edu.hk and his webpage is www.cityu.edu.hk/seem/kltsui/.